Abstract code: DP5

Multi-hazard risk assessment in Fella Basin (Italy) using historical hazard inventory and GIS

Lixia Chen[1,3], Haydar Hussin[1], Roxana L.Ciurean[2], Thea Turkington[1], Cees van Westen [1], Diana Chavarro[1] , Dhruba Shrestha[1]

[1]Faculty of Geo-Information Science and Earth Observation (ITC), University of Twente, Enschede, Netherlands

[2] Department of Geography and Regional Research, Geomorphic Systems and Risk Research Unit, University of Vienna, Vienna, Austria

[3] Institute of Geophysics and Geomatics, China University of Geosciences, Wuhan, China

Corresponding author details:
Lixia Chen, Faculty of Geo-Information Science and Earth Observation (ITC), University of Twente. E-mail: l.chenlixia@utwente.nl

Keywords:
Multi-hazard risk assessment, Debris flows, Floods, Fella River, Italy, Vulnerability

INTRODUCTION

Hydro-meteorological hazard is the process or phenomenon of atmospheric, hydrological or oceanographic nature that may cause loss of life, injury or other health impacts, property damage, loss of livelihoods and services, social and economic disruption, or environmental damage (UNISDR, 2009a). Such hydro-meteorological conditions also can be a triggering event for the occurrence of debris flows, rock falls, avalanches, and shallow or deep-seated landslides in mountain areas.

Compared to single hazard risk assessment, multi-hazard research can satisfy the demand of risk management of mountainous areas prone to high-intensity rainfall and subsequent flood or slope instabilities. Because of the difference in physical mechanism or intensity of each hazard type, the combination of multi-hazards is difficult. Meanwhile, the importance of the relations between hazards is increasingly acknowledged within multi-hazard research (Kappes et al., 2012, Timo Tarvainen, 2006). The impact of these hazards, such as exposure, loss or risk, in a multi-meteorological hazard risk assessment are relatively difficult to analyze, because of the interrelation of the hazards, and the difficulty in expressing landslide hazards in terms of intensity maps for different return periods. This type of analysis is important for risk mitigation investments and relative decisions should be made both for multiple or single types of hazards, and for prioritizing the most risky areas encountered with respect to the limited budgets for risk mitigation. This study presents the results of a multi-hazard risk assessment. The Fella river basin in NE Italy is used as a pilot study area in the EU FP7 ITN CHANGES, and EU FP7 Copernicus INCREO projects, which aim to develop an advanced understanding of how global changes, related to environmental and climate change as well as socio-economical change, will affect the temporal and spatial patterns of hydro-meteorological hazards and associated risks in Europe; how these changes can be assessed, modelled, and incorporated in sustainable risk management strategies, focusing on spatial planning, emergency preparedness and risk communication. Accordingly, the main objective of this paper is to assess, model the temporal and spatial changes of multi hazard in this area.

METHODOLOGY AND DATA

Methodology

The flow chart of the methodology is shown in Figure 1. In order to support the local government to better manage and reduce hazard risk, the quantitative multi-hazard risk assessment was carried out using a historical landslide inventory and GIS modelling.

Based on historical landslide inventory data and rainfall events from 1976 to 2011, the return period for each class of hazard events was determined with extreme value distribution analysis with daily rainfall and 40 days accumulative precipitation. The catchment characterization was carried out based on the geological, topographical and rainfall data. Discharge for each return period was calculated by means of base flow and run off analysis. Based on this process, flood boundaries, water depth, and velocity maps were obtained for three return periods through hydraulic modelling with Hec-RAS. Flood risk assessment was then conducted by using overlay of a series of modelled flood intensity maps for different return periods with building footprints and vulnerability curves obtained from the literature. A flood loss estimation was subsequently carried out using GIS.

A landslide hazard map was generated from a five-class landslide susceptibility map and rainfall event magnitude. Run-out modelling was carried out by using Flow-R software, a modelling software that uses a GIS empirical distribution model to probabilistically estimate the flow path and run-out extent of gravitational mass movements at regional scales. Four steps were conducted for the model: (1) Source area identification;(2) Parameterization of the run-out model; (3) Debris flow hazard intensity modelling;(4)Spatial probability calculation. By using the Weights-of-evidence method, a five class susceptibility map was generated based on five factors including lithology, land-cover, altitude, plan curvature and slope. The susceptibility map was utilized as the source area selection for the landslide run-out modelling in the Flow-R software to generate intensity indicators (kinematic energy as indicator of impact pressure). Areas with very high susceptibility were then chosen as one factor for landslide initiation source area identification, which is required as an initial input for run out modelling in Flow-R software. Besides this, a criteria set is required in order to determine the pixels that are chosen as source areas to release the flows on the DEM. The criteria were chosen partly based on previous studies (Blahut et al., 2010, Horton et al., 2013, Horton et al., 2008, Kappes et al., 2011) but were also updated specifically for the Fella River basin. Planar curvature lower than -4/100 m^{-1} and slope values above 15° was then added as the other two determination factors for source area identification. Historical landslide areas belong to different event scenarios were finally added. Two parameters were required to model the run-outs for each return period in the Flow-R model: (1) the minimum travel angle and (2) the maximum velocity. These two parameters were back calibrated based on 1 or 2 historical landslides for each event scenarios. The back calibration included 2 sets of parameters, a minimum and maximum for each return period in order to include uncertainty in the parameter values which is translated in an uncertainty range in run-out extent and probability values. The method is further explain by Hussin et al. (2014).

The spatial probability of the debris flow hazard areas was determined by overlaying the modelled debris flow areas with the actual debris flow inventories that correspond to these return periods, and for those areas that were not affected by historical debris flow a spatial probability was calculated as the ratio between the historical inventory areas and the modelled areas, resulting in lower spatial probabilities for lower return periods that have fewer debris flow events. For the modelled flood intensity areas, and for the areas that were affected by historical debris flows, a spatial probability value of 1 was used. Vulnerability curves were generated, partly based on available curves from the literature, and partly based on actual damage information from the 2003 event, combined with expert opinion. Curves were made for debris flow impact pressure, and flood water depth, for 8 building types (which are a combination of the material type and the number of floors). Curves were made for the physical vulnerability for buildings, and for population. The hazard intensity data for each building and hazard return period in combination with the vulnerability curves were used to

convert them into vulnerability data. Losses were then calculated for each building and hazard return period by multiplying the vulnerability, the spatial probability and the amount. The amount is related to the minimum and maximum building values in the case of economic losses, and for the minimum and maximum number of persons per building (taking a normal scenario and a tourist season scenario) to calculate the population loss. The risk was analysed by aggregating the loss data per building, and hazard return period for administrative units within the study area, and for the entire study area (which includes the towns and villages between Pontebba and Ugovizza). Minimum values for temporal probability (1/return period) were used in combination with minimum values of loss (multiplying minimum values of intensity, and amount) to generate minimum risk curves, and maximum values to generate maximum risk curves. The multi hazard including landslide and river flood was analysed by comparing or combining the risk results of these two hazard types. After overlaying these two risk maps under each return period, the risk value was then calculated for each building. If one building was influenced by both these two hazards, the maximum risk value of both was taken. After this combination, the multi hazard risk was generated as risk curves and risk maps by administrative units.
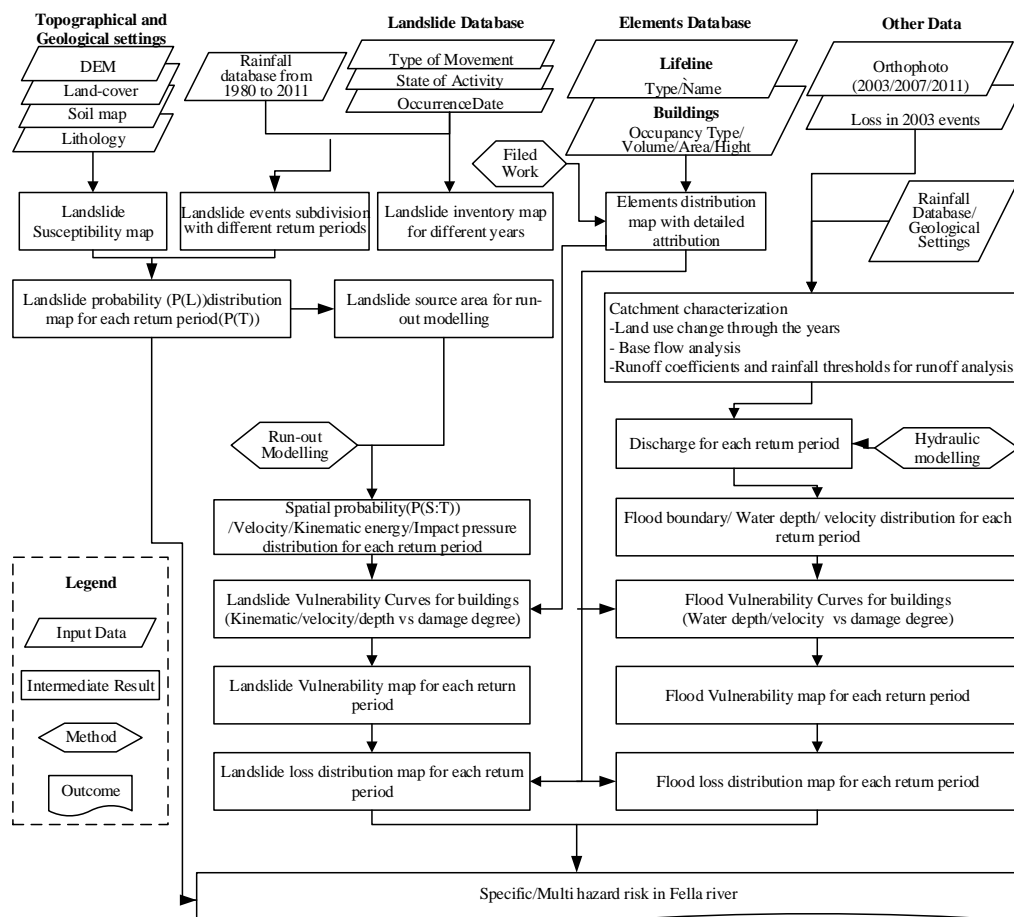

Figure 1: Methodology for multi hazard risk assessment in Fella Basin, Italy

Study area and data

The Fella River study area is located in the province of Udine, within the Friuli-Venezia Giulia region, in the north-eastern part of the Italian Alps (Figure 2). It covers 247 km^2, with five communes including Pontebba, Dogna, Malborghetto-Valbruna, Tarvisio from the West to the East. The elevation of the area ranges from 426m along the Fella River to 2753m.

The landscape is predominantly mountainous and the land cover is dominated by broad-leaf and conifer forests. Geologically the area is underlain mostly by Permian and Triassic formations, consisting of mainly dolomite, limestone and calcareous-marls. Quaternary deposits are mainly distributed in the form of debris accumulation fans, glacial and alluvial deposits along the valley. Complex geological structures including monoclines, bends and faults contribute the fractures of bedrocks, which therefore became as an important intrinsic factor for debris flow and landslides in the area. The Fella River area is affected mainly by flood and landslides. Geological survey before 2007 indicates that most significant failures was recognized in Udine, the province of the study area (Paolo,et. al, 2007). Rainfall produced by the August 2003 storm resulted in severe flooding and debris flows throughout the Fella river basin.

RESULTS
Landslide inventory mapping and scenarios determination
Landslide inventories were used from the IFFI project, and the AVI project. However, many of them didn't have clear information on the date of occurrence. Therefore a substantial reanalysis of this data was done using satellite images and airphotos. In the study area, the inventory map contains 1018 landslides, covering a total area of 39.7 km^2, 21.8% of the study area. Landslides range in size from 32 m^2 to 0.94 Km^2. As the map shows (Figure 2): (i) 132 slopes are affected by widespread rockfall and toppling, covering a total area of 19,48 Km^2 ;(ii) 49 slopes are affected by widespread shallow landslides, covering a total area of 1,65 Km^2; (iii) 423 debris flows, including both source area and deposit area, cover a total area of 16,43 Km^2; (iv) 361 slides, including both rotational and translational types, cover a total area of 1,69 Km^2; (v)18 rock falls, covering a total area of 0,332 Km^2 . From these figures it is clear that the study area is mostly prone to rockfall and toppling, debris flow and shallow landslides. These types of movement represent the vast majority of the landslides recognized in Fella area. The state of activity is also considered in this map (Figure 2). The classification was based on Varnes(1996). 76 landslides were identified as dormant, reactivated and stabilized. But most of them were either recorded as active/reactivated/suspended or with unknown data.
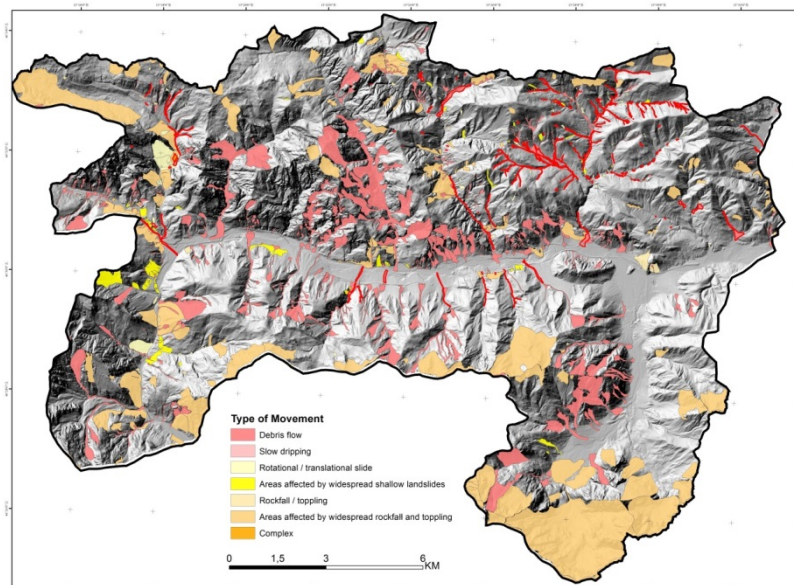

Figure 2: Distribution of landslides with different type of movement in Fella river and location map.

According to landslide occurrence or reactivation dates in the original inventories, multi temporal maps from 1996 to 2011 were extracted from the above landslide inventory map. One landslide can therefore have two different dates of occurrence. One is for the initial

occurrence and the other for reactivation. Some landslide polygons in some years can therefore overlap by those from another year. For example, a landslide in map 1996 can also be on map 2003, which means the landslide was reactivated in 2003 after the possible first time of instability in 1996. Ten individual maps from 1996 to 2011 were made for the study area. These maps can be used for spatial and temporal analysis of landslide distribution, exposure and damage analysis. About 19 landslide events were defined and four scenarios were determined according the daily precipitation records. In the records of each year, landslides could be found to be concentrated in some dates, especially in the summer season. Because of the available data of landslide dates in the database, event-based landslide inventory maps were then generated. As that triggering event may be an earthquake, rainstorm or prolonged rainfall period, or rapid snowmelt event, the time when slope failures were triggered usually focused on some day or during a special period. It can be included that the event from 25/8/2003 to 1/9/2003 was the most serious one triggered by rainfall, which caused 631 landslide occurrences in the area, with about 2.5 landslides per square kilometer.

In the landslide inventory, there is no distinction between rapid landslides, such as debris flows, and shallow landslides. Therefore, rainfall thresholds were applied using 1 day and an antecedent period of 40 days. For the antecedent period, 40 days was the time period over which most of the landslide events had higher than normal rainfall amounts. According to the above result of typical landslide event return periods, the non-frequent events are classified to be major, moderate and minor separately with 100 to 500 years, 25 to 100 years, 10 to 25 years return periods(See table 1). The large variation indicates the uncertainty based on the magnitude-frequency analysis. And for the more frequent events in other years except 2003, 1996 and 2011, the return period was determined to be 1 to 10 years. For each scenario, the number and area of recorded landslides and debris flows were statistically analyzed. It shows that there is a general decreasing tendency both in numbers and areas for these for scenarios. Meanwhile, the amount of triggering rainfall also became smaller form major to minor scenario.

Table 1: Scenario classification and return periods

Scenario Class		Major	Moderate	Minor	Frequent
Return Period(years) (with 80% confidence bound)		100-500	25-100	10-25	1-10
Representative event	Date	25/8/2003~1/9/2003	22/06/1996	06/12/2011	1/9/2005
	1d Rainfall(mm)	354,6	192,2	154.4 (19/06/2011*)	/
	Return Period (Years)	133	26	14	/
Historical years		2003	1996	2011	Other years
Recorded landslides	Number	631	200	10	14
	Area($\times Km^2$)	14,551	2,870	0,617	0,093
Debris flows	Number	144	137	7	5
	Area($\times Km^2$)	6,79	2,02	0,58	0,05

Debris flow run-out modelling and spatial probability assessment

Accordingly, 8 maps with different run-out spatial probability were modelled and used as the input data for landslide intensity calculation. Linear functions were generated and imported for the transferring of probability to intensity. They were obtained based on two factors: (1) the spatial distribution and variation of the probability values within the debris flow morphology (from the debris flow channels and transportation zones to the end of the deposit

zones at the debris fans) and (2) the estimated impact pressures in the field based on damage assessments of past events. Table 2 shows the model parameters used to produce the run-out maps for each return period. The maximum impact pressure found in the most extreme event with the lowest return period (100-500y) was 35 KPa, which caused the total destruction of several houses. Therefore, the maximum impact pressure for all other return periods does not exceed 35 KPa and is considered a cut-off value. Figure 5 shows the run-out probability – impact pressure transfer curves. As the severity for events with lower return periods increases, so does the impact pressure. Therefore, the minimum and maximum run-out maps of each return period is assigned a different transfer curve. A run-out probability of 0.5 gives an impact pressure of 35 KPa for a major event, while the same probability for a frequent event will have an impact pressure of 17.5 KPa. The run-out polygons from the historic inventory of each return period that did not correspond to the modelled run-out extents were also included in the intensity maps. These were assigned average impact pressure values calculated from building locations which overlapped with the modelled run-outs and are shown in the table 3. Figure 3 shows the debris flow run-out result for each return period.

Table 2: Parameters used run-out modelling for different return period

Event (Return Period)	Range	Travel angle (degrees)	Velocity (m/s)	Average impact pressure (KPa) for non-modeled historic debris flows
Major (100-500y)	Max	13	15	5.80
	Min	15	10	5.00
Moderate (25-100y)	Max	15	10	4.67
	Min	18	8	3.45
Minor (10-25y)	Max	17	8	3.28
	Min	20	8	3.33
Frequent (1-10y)	Max	20	5	3.96
	Min	22	4	3.48

Flood hazard analysis

To obtain the river flood intensity, two main research works were conducted: (1) a hydrological study of the area and (2) a hydraulic modelling of the flood for different possible discharges with associated return periods. One of the main problems in this study turned out to be the absence of a rating curve. A frequency analysis of discharges was performed at the catchment outlet (C400 station) given the available 3-years of hourly discharges (2006-2008) provided by the Regione FVG. In order to determine the return period of modelling discharges, the storms recorded at the Dogna catchment that resulted in quick flow at the main channel were correlated with the peak discharges during the 3-year data on hourly bases. The frequency of the same storms obtained from the long historical series of the same stations was finally assigned to the peak discharges in order to provide a return period to the flood analysis. Such return periods are only valid for the catchment outlet at Dogna and a proportional flow based on the drainage area of every sub-catchment was modelled for flood-mapping purposes along the main channel from Ugovizza to Dogna. The lack of available rating curves or direct measurements of discharges introduced high uncertainty to the frequency analysis of the floods and therefore the results should be considered with caution. The hydraulic modelling for flood mapping was performed using HecRAS 4.1 and its GIS-assisted version GeoHecRAS (ArcGIS 10.1). The bathymetry of the river and correspondent topography of the flood plain was obtained from Lidar data at 1m resolution. Due to model high computational demands, the river was divided in 2 reaches: the Northern corridor, running East-West from Ugovizza to Pontebba, and the Mid corridor (denominated in that way considering the additional corridor From Dogna to Moggio Udinese), running North-South from Pontebba to Dogna.

Figure 3: Debris flow run out result for each return period.

Figure 4: Flood depth maps for three return periods (above: 3-5 years, Middle: 40-50 years, and below: 300-400 years).

The model showed a river regime mainly supercritical with rapid flows and high shear forces. Model outputs shown in figure 4 include flood boundaries, inundation depths, and velocity and stream power maps for discharges ranging from 100 to 700 m3/sec (at Pontebba, C331). Sources of difficulty for the modelling include the large amount of roads/railways/highways intersections affecting the Lidar data accuracy and the flow behaviour, and the sinuosity of the river bed as a limitation of a 1-D hydraulic model.

Elements at risk

Buildings inventory and database update

Based on the initial building footprint map with building locations, geometry and type, a field survey was carried out for more detailed information collection. Consequently, the inventory was updated in the ILWIS software with the following attributes: number of floors, materials of construction, occupancy type, using Open Street Map and Google Street View. Field work was then carried out in the area along the main valley for checking and updating. Removed or abandoned buildings which were on the initial map were removed and other buildings were assigned an attribute to show the change. The final building footprint map was generated with the following attributes: location, geometry, number of floors, materials of construction and occupancy type. The final inventory map contains 4778 buildings. Six types of buildings material were classified including masonry, wood, concrete, brick, metal and wood. The main type of material is masonry and the main occupancy type residential buildings. The building occupancy types are categorized in 16 classes (Figure 5). The residential and residential storage buildings are the most frequent occupancy types, with 39.5% and 41.8% respectively.

Evaluation of population and value for each building

Statistical data in the study area was obtained on the population and number of beds in each commune. To get the data for each building, the building occupancy type, area and number of floors were taken into account. Two population scenarios were used: tourist and non-tourist seasons, and population numbers per building were calculated. Because of the large difference in population between non-dwelling buildings and dwellings (houses), the calculation for buildings (e.g. Apartment) was carried out for the dwellings only. The average area per house was used to calculate the number of dwellings per multi-storey apartment building. The number of residents per dwelling was calculated by dividing the number of residents per commune (separate for each scenario) with the number of dwellings. Finally, the number of residents per building was calculated by multiplying the number of dwellings with the number of residents per dwelling. Only residential buildings were used for estimating the spatial distribution of people in the study area. The results show that in Malborghetto-Valbruna, Pontebba and Tarvisio communes the population increases whereas in Dogna, the calculated number of people for both touristic and non-touristic season remains almost constant. The building value was obtained from the Italian Revenue Agency (Agenzia delle Entrate, http://www.agenziaentrate.gov.it), for the second semester of 2013. The buildings were classified per cadastral zone according to the Real Estate Observatory data (Osservatorio del Mercato Immobiliare, Agenzia Entrate – OMI). The minimum and maximum market value for each building was obtained by multiplying the corresponding unit value (€/msq) with the building area and number of floors.
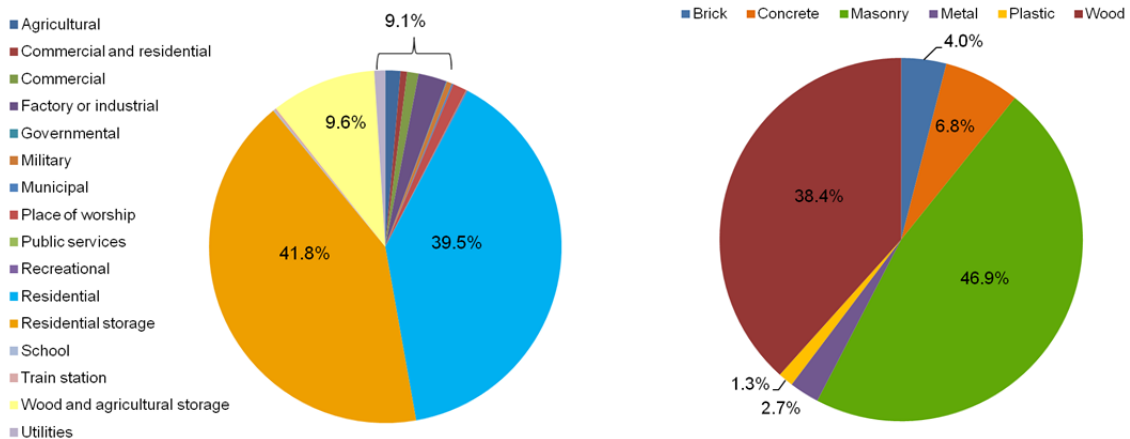
Figure 5: Percentage distribution of building occupancy (left) and construction types (right)

As each building in the inventory has a minimum and a maximum value assigned, it was possible to calculate the variation in price for buildings grouped per value range. A large heterogeneity of buildings was encountered (in terms of use, material of construction, occupancy type, etc.) for value categories of less than 10.000, 10.000 - 50.000, 500.000 – 800.000, 800.000 - 1.250.000 Euros, although for the latter two the number of buildings is significantly lower compared with the former ones.

Exposure and risk assessment
The direct input maps for the exposure analysis consist of the flood depth maps for 4 different return periods (3-5 years, 40-50 years, 300-400 years, and 400 – 700 years), the debris flow run-out maps for 4 different return periods (1-10 years, 10-25 years, 25-100 years and 100-500 years), and the building map (with attributes related to the occupancy type, construction type, minimum and maximum building value, and population information for two scenarios). The maximum intensity for each return period and hazard type for each building was analysed in GIS. Summary information on the number of exposed buildings for different communes and hazards were generated. The risk was represented by loss curves, plotting losses against annual probability (Westen et al., 2002). Figure 6 shows the exposure of economic value and population by debris flow and flood. The general tendency that low probability event will cause high exposure or risk is the same both to flood and debris flow hazard. But differences exist when comparison was made between flood risk and debris flow. Figure 7 shows that economic risk from flooding is much higher when encountered with a same probability above 0.05 or return period shorter than 20 years, whereas population risk shows an opposite performance. Thant means high frequency debris flow occurs in Fella and more easily causes casualties than physical damages. But once flood event occurred, both population and economic loss would exist and much higher than it from debris flow. Such risk characteristics in Fella should be taken into consideration when short or long period hazard or land use planning is carried out in future.
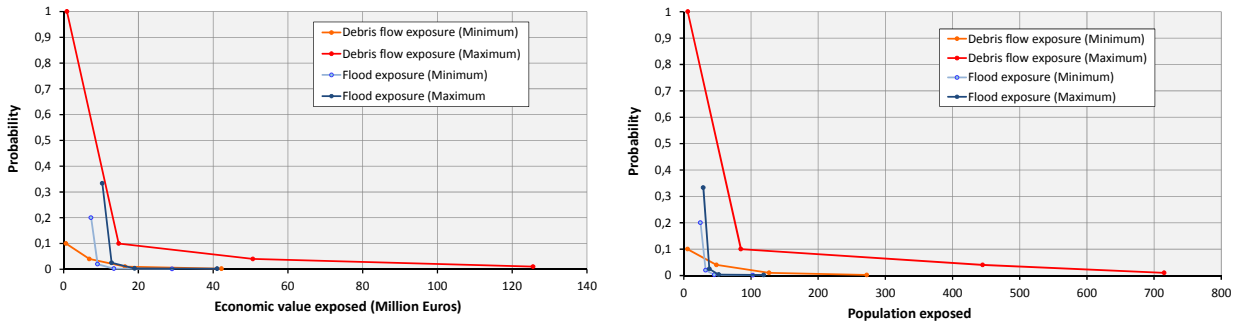
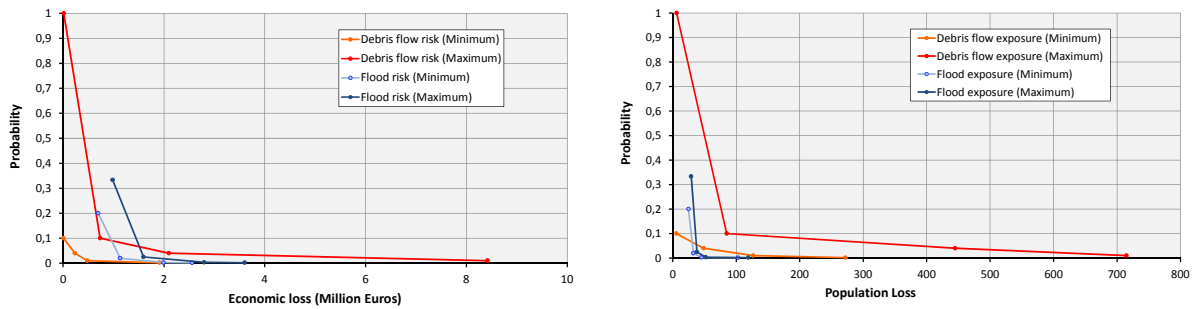Figure 6 Exposure curves for economic value (left)and population (right)

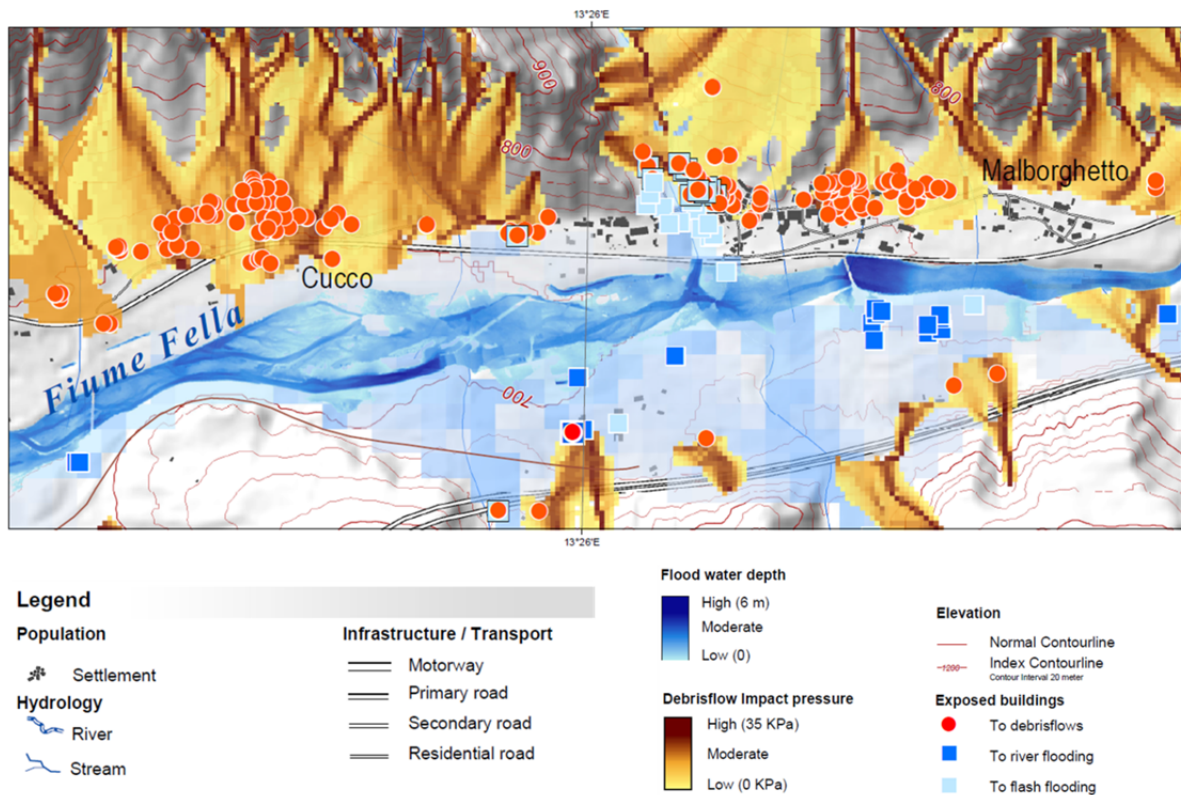Figure 7: Risk curves by plotting economic loss (left) and population (right) against annual probability

Figure 8: Fragment of the exposure map, showing the buildings exposed to debris flows, river flooding and flash flooding.

CONCLUSIONS

Quantitative risk information can be an important basis for hazard risk mitigation and other management measures in Fella River, Italy. In addition, debris flow potential influence area, intensity and flood inundation area or depth can also be indicators for land use planning in such meteorological hazard prone areas.

Flash flood hazard should be another type of hazard that should have been included in this study. Due to the limitations in scale and quality of available soil data, flash food modelling could not be carried out at a satisfactory level in this study. Debris flow run-out modelling results shows a good performance for the potential influence area, but not well for intensity distribution. It will be improved by further analysis based on geological condition classification, and further calibration and comparison of regional scale run-out modelling with local scale analysis. Further work is also needed to generate more reliable vulnerability curves for debris flows and flooding in an alpine setting. But because of the time limitations, the curves were taken from literatures which may be not very suitable for the elements-at-risk in the area. Back analysis will be carried out later aiming at improving vulnerability curve definition based on historical damages and debris flow run-out modelling. Thus, hazard intensity and more suitable vulnerability curves can therefore contribute for more reasonable economic or population risk results.

ACKNOWLEDGEMENTS

REFERENCES

United Nations International Strategy for Disaster Reduction. Terminology. Geneva, Switzerland: UNISDR; 2009. http://www.unisdr.org/we/inform/terminology (Access date 13th September 2011)

BLAHUT, J., HORTON, P., STERLACCHINI, S. & JABOYEDOFF, M. 2010. Debris flow hazard modelling on medium scale: Valtellina di Tirano, Italy. *Nat. Hazards Earth Syst. Sci.,* 10**,** 2379-2390.

HORTON, P., JABOYEDOFF, M. & BARDOU, E. 2008. Debris flow susceptibility mapping at a regional scale. *4th Canadian Conference on Geohazards***,** 399-406.

HORTON, P., JABOYEDOFF, M., RUDAZ, B. & ZIMMERMANN, M. 2013. Flow-R, a model for susceptibility mapping of debris flows and other gravitational hazards at a regional scale. *Nat. Hazards Earth Syst. Sci.,* 13**,** 869-885.

KAPPES, M. S., KEILER, M., VON ELVERFELDT, K. & GLADE, T. 2012. Challenges of analyzing multi-hazard risk: a review. *Natural Hazards,* 64**,** 1925-1958.

KAPPES, M. S., MALET, J. P., REMAÎTRE, A., HORTON, P., JABOYEDOFF, M. & BELL, R. 2011. Assessment of debris-flow susceptibility at medium-scale in the Barcelonnette Basin, France. *Nat. Hazards Earth Syst. Sci.,* 11**,** 627-641.

TIMO TARVAINEN, J. J., STEFAN GREIVING 2006. spatial pattern of hazards and hazard interaction in Europe. *Schmidt_Thome P (ed) Natural and Technological Hazards and Risk Affecting the Spatial Development of European Reagions.,* 42**,** Geological Survey of Finland:83-91.

WESTEN, C. J., MONTOYA, L., BOERBOOM, L. & BADILLA COTO, E. 2002. Multi-hazard risk assessment using GIS in urban areas: a case study for the city of Turrialba, Costa Rica.

PAOLO MANCA, FABRIZIO KRANITZ,SARA OBERTI , CHIARA PIANO. Il Progetto IFFI come base informativa per la redazione dei piani stralcio:l'esempio della Regione Friuli Venezia Giulia. Rend. Soc. Geol. It., 4 (2007), Nuova Serie, 63-73, 11 ff.